HHS Public Access

Author manuscript

Neuron. Author manuscript; available in PMC 2017 September 07.

Published in final edited form as:

Neuron. 2016 September 7; 91(5): 1154–1169. doi:10.1016/j.neuron.2016.07.032.

Hunger-dependent enhancement of food cue responses in mouse postrhinal cortex and lateral amygdala

Christian R. Burgess[1,*], **Rohan N. Ramesh**[1,2,*], **Arthur U. Sugden**[1], **Kirsten M. Levandowski**[1], **Margaret A. Minnig**[1], **Henning Fenselau**[1], **Bradford B. Lowell**[1,2], and **Mark L. Andermann**[1,2]

[1]Division of Endocrinology, Beth Israel Deaconess Medical Center, Harvard Medical School, Boston, MA, USA, 02215

[2]Program in Neuroscience, Harvard Medical School, Boston, MA, USA, 02115

Summary

The needs of the body can direct behavioral and neural processing towards motivationally relevant sensory cues. For example, human imaging studies have consistently found specific cortical areas with biased responses to food-associated visual cues in hungry subjects, but not in sated subjects. To obtain a cellular-level understanding of these hunger-dependent cortical response biases, we performed chronic two-photon calcium imaging in postrhinal association cortex (POR) and primary visual cortex (V1) of behaving mice. As in humans, neurons in mouse POR, but not V1, exhibited biases towards food-associated cues that were abolished by satiety. This emergent bias was mirrored by the innervation pattern of amygdalo-cortical feedback axons. Strikingly, these axons exhibited even stronger food cue biases and sensitivity to hunger state and trial history. These findings highlight a direct pathway by which the lateral amygdala may contribute to state-dependent cortical processing of motivationally relevant sensory cues.

In Brief

Burgess, Ramesh, and colleagues demonstrate a hunger-dependent response bias towards food-associated visual cues in mouse postrhinal cortex, but not primary visual cortex. Chronic axonal calcium imaging and circuit mapping implicate lateral amygdala afferents in biasing postrhinal processing towards motivationally relevant cues.

Correspondence: Mark L Andermann, Division of Endocrinology, Diabetes, and Metabolism, Beth Israel Deaconess Medical Center, Center for Life Sciences, CLS701, 330 Brookline Ave, Boston, MA 02215, manderma@bidmc.harvard.edu.

*These authors contributed equally to this work

Author Contributions

CRB, RNR and MLA designed experiments and analyses, and wrote the manuscript. CRB and RNR performed two-photon imaging experiments. RNR analyzed calcium imaging data with assistance from CRB. CRB, AUS, KML, and MAM performed and analyzed anatomy experiments. HF and BBL performed and analyzed electrophysiology experiments.

Introduction

Our understanding of the neural mechanisms underlying sensory attention has benefited from experiments involving explicit instructions to focus on particular sensory cues (Posner, 1980). Yet, in practice, it is the changing needs of the body that often guide our attention to motivationally relevant stimuli. For example, humans attend more to food cues during hungry *vs.* sated states (Higgs et al., 2012). Accordingly, a large number of human neuroimaging studies consistently demonstrate hunger-dependent enhancement of neural responses to visual food cues *vs.* non-food cues in temporal association cortex, but not in early visual cortex (Cornier et al., 2007; LaBar et al., 2001). Interestingly, these neural biases towards food cues are exaggerated in obese subjects (Yokum et al., 2011), even in the absence of caloric deficits, and their magnitude can predict future clinical outcomes, including weight gain (Cornier et al., 2013; Sun et al., 2015). While these and other human imaging studies highlight the importance of understanding the neural biases elicited by basic need states, little is known about the cellular-level cortical and subcortical processes underlying motivational biases in sensory processing.

The lateral amygdala (LA) and basolateral amygdala (BLA) have established roles in forming cue-outcome associations and updating the perceived value of environmental stimuli (Baxter and Murray, 2002; LeDoux, 2003; Morrison and Salzman, 2010; Paton et al., 2006). Specifically, lesions of the LA/BLA prevent learning and identification of motivationally relevant stimuli (Blair et al., 2005; Holland and Gallagher, 2003). Intermingled BLA neurons have been shown to encode either the positive or negative value of learned visual cues (Baxter and Murray, 2002; Morrison and Salzman, 2010; Paton et al., 2006), and to encode stimulus value at the time of decision making (Jenison et al., 2011). Amygdala-dependent assignment of value depends, at least in part, on the motivational state of the animal, as demonstrated by reinforcer-devaluation experiments (Hatfield et al., 1996; Johnson et al., 2009). Paired recordings in BLA and temporal cortex suggest that amygdalo-cortical connectivity may enhance the flow of salient sensory information (Paz et al., 2006), and behavioral experiments suggest the importance of amygdalo-cortical connectivity in palatability estimation (Fontanini et al., 2009) and other behaviors (Sparta et al., 2014). In addition, the aforementioned neuroimaging studies consistently identify the LA/BLA as part of the network involved in hunger-dependent enhancement of responses to food cues (LaBar et al., 2001; Sun et al., 2015). Studies across multiple species have shown that the LA/BLA send glutamatergic feedback projections to temporal cortical areas (Pitkanen et al., 2000). However, the nature of state-dependent information relayed by these direct projections *vs.* indirect pathways to cortex remains unclear. We hypothesized that direct amygdalo-cortical afferents would show pronounced hunger-dependent response biases to food cues, and that cortical neuron biases would co-vary with the density of amygdalo-cortical afferent input.

To overcome obstacles involving repeated monitoring of cellular responses across slowly-changing motivational states, we used two-photon calcium imaging to record the activity of hundreds of individual neurons or long-range amygdalo-cortical axons across hours and days, and across states of hunger and satiety. We investigated hunger-dependent sensory processing in mice performing a Go/NoGo task involving discrimination of food-predicting cues from other visual cues, while imaging neurons in either primary visual cortex (V1),

postrhinal cortex (POR, a rodent homologue of human parahippocampal gyrus and part of temporal association cortex; Beaudin et al., 2013), or long-range feedback axons from LA to POR ($LA^{\rightarrow POR}$). While a subset of neurons in V1 did demonstrate state-dependent modulation of neural activity, a population response bias towards food cues was only evident in POR, and not in V1. As in humans, this food cue bias was abolished following satiation. Further, we found that $LA^{\rightarrow POR}$ axons received subcortical inputs as well as dense and specific inputs from POR neurons. Strikingly, $LA^{\rightarrow POR}$ axons demonstrated particularly pronounced food cue biases, sensitivity to hunger state, and sensitivity to recent trial/reward history. Together, our data are consistent with a role for $LA^{\rightarrow POR}$ axons as a subcortical source of top-down feedback that flexibly biases sensory processing in association cortex towards motivationally relevant cues.

Results

Robust discrimination of food cues from other visual cues in head-fixed mice

We trained food-restricted mice (~85% of free-feeding weight) in a Go/NoGo orientation discrimination task (Figure 1A–C). Following several sessions of habituation to head-fixation and placement on a rotating trackball, we presented visual cues (square-wave drifting gratings) on an LCD monitor for 2 s, followed by a 2 s response window, and a 6 s inter-trial interval. Mice were trained to discriminate between a food cue (FC; 0°), a quinine cue (QC; 270°), and a neutral cue (NC; 135°). Licking during the response window following the FC, QC, or NC resulted in delivery of high-calorie liquid food (5 μL of Ensure), an aversive bitter solution (5 μL of 0.1 mM quinine), or nothing, respectively (Figure 1C). Mice typically learned this task in ~2–3 weeks, and maintained consistently high performance (>85% hit rate; Figure 1D; Figure S1B–C) across tens of sessions (~800 trials/session), facilitating comparison of cue-evoked neural responses across days and across mice.

Food cue responses of V1 and POR neurons in behaving mice

We used two-photon calcium imaging to record visual responses of neurons in layer 2/3 of either primary visual cortex (V1) or postrhinal association cortex (POR). Following cranial window implantation, we localized monocular regions of awake mouse V1 or POR using retinotopic stimulation and widefield imaging of intrinsic autofluorescence, and targeted these regions with injections of AAV-hSyn-GCaMP6f (Andermann et al., 2011; Chen et al., 2013; Garrett et al., 2014). We confirmed our injection location via two-photon calcium imaging (Figure 1E). Despite the overlap in axonal inputs to POR from retinotopically distinct regions of V1 (Wang and Burkhalter, 2007), retinotopic organization of POR at cellular resolution was quite sharp. POR was the most lateral retinotopically-defined visual area we could observe. As a first step, we mapped visual responses in POR of naïve, untrained, awake mice (n=4 mice, n=14 fields-of-view, n=1049 neurons), and found that many POR neurons were visually responsive and demonstrated sharp orientation tuning (Figure S2A–B).

We then obtained simultaneous recordings of cue-evoked responses across multiple sessions of discrimination behavior from neurons in V1 and POR of well-trained mice (V1: n=4

mice, n=372 neurons, n=3–8 sessions/field-of-view, 31 sessions total; POR: n=4 mice, n=317 neurons, n=4–12 sessions/field-of-view, 34 sessions total). Individual neurons in both areas showed robust responses to at least one visual cue (see Figure 2A–C and S3A for example neurons in POR and V1, respectively). Neurons were deemed visually responsive if they had a significant response (see Supplemental Experimental Procedures) during one or more visual cues. To minimize possible contributions of lick-related activity, we assessed responsivity using data up to 100 ms prior to the first lick in each trial (Figure 2C; median time to 1st lick: 1.8 s post cue onset). Using these conservative criteria, similar fractions of V1 neurons and POR neurons showed significant responses to presentation of at least one of the three visual cues (V1: 27%, 102/372; POR: 33%, 105/317; see Figure 2D–E). Response timecourses of all visually driven neurons to all three visual cues are shown in Figure 2D.

We found a strong bias towards food cue preferring neurons in POR of well-trained, food-restricted mice, but not in naïve mice. In well-trained mice, more than twice as many visually responsive POR neurons preferred the FC as compared to the QC and the NC (Figure 2E; POR: $p<0.05$, FC *vs.* QC/NC; FC: 52%; QC: 21%; NC: 27%; Tukey's HSD multiple comparisons test among proportions). By contrast, visually responsive POR neurons recorded in naïve, untrained mice (276/1049 of recorded neurons), showed no bias in the proportions preferring the FC (0°), QC (270°), or NC (135°) orientations (Figure S2A–B; $p>0.05$; 0°/180°: 29%; 90°/270°: 28%, 135°/315°: 25%, Tukey's HSD). This suggests that the FC bias in trained mice is due to the higher incentive salience of food cues after learning.

In V1 of trained mice, no significant difference was evident between the FC and QC. However, approximately half as many neurons responded to the NC as to the FC or QC (Figure 2E; V1 $p<0.05$ FC/QC *vs.* NC; FC: 40%; QC: 38%; NC: 22%; Tukey's HSD), likely due to the fact that in untrained mice, fewer V1 neurons are responsive to the oblique orientation of the NC (135°) *vs.* the cardinal orientation of the FC (0°; Roth et al., 2012).

To assess population-level neural response biases, we normalized the response tuning curve of each visually responsive neuron (cue-normalized $\Delta F/F$), and then averaged across all cells. We observed an emergent bias in the population response towards the food cue in POR (Figure 2F; POR: FC *vs.* QC: $p<0.001$; FC *vs.* NC: $p<0.001$; QC *vs.* NC: $p=0.9$; V1: all p's>0.05, 2-way ANOVA with Tukey *post hoc* test). Thus, not only did a larger fraction of visually responsive cells prefer the food cue in POR, but this bias was also reflected in the pooled population activity across POR neurons. Using the same analysis in naïve, untrained mice, there was no bias to the 0° FC (Figure S2C; $p>0.05$ for all comparisons to 0°, Kruskal-Wallis). Despite the lack of an inherent bias to a given orientation in naïve mice, we reproduced these FC bias findings in POR recordings from a separate cohort of mice (n=3) trained with FCs at other orientations (135° or 270°; Figure S4). As in human neuroimaging studies, these data suggest that mouse higher-order visual cortical areas, but not V1, show net population biases towards learned, motivationally relevant cues.

Importantly, the population response bias we observed in POR was evident shortly after stimulus onset, well before any licking occurred. Trials containing licking in the first 500 ms following, or in the 1 s prior to, cue onset were removed from all analyses (see Figure S3D),

and only activity up to 100 ms prior to the first lick was used to estimate the response on each trial. We reproduced these findings even when restricting analyses to data acquired up to 300 ms or 500 ms prior to the first lick on each trial (Figure S3E). Additionally, while the median latency to first lick was ~1800 ms after cue onset, a significant population bias to the FC emerged much earlier, ~360 ms after cue onset (Figure S3E–F; FC *vs.* QC: p=0.006; FC *vs.* NC: p=0.004; QC *vs.* NC: p=0.99). While we did observe a small number of visually responsive POR neurons whose activity also correlated, on a trial-by-trial basis, with licking behavior (see Figure 8 and Figure S7), a significant POR population response bias to the FC persisted following removal of these neurons from the analysis (FC *vs.* QC: p=0.02; FC *vs.* NC: p=0.001; QC *vs.* NC: p=0.99; data not shown).

The responses of primary sensory cortical neurons are known to be fairly stable across days in untrained (Mank et al., 2008) or trained (Chen et al., 2015; Poort et al., 2015) mice, while the excitability of hippocampal neurons varies substantially across days (Ziv et al., 2013). However, little is known about across-day stability of representations in intervening regions such as POR, which is both a higher visual cortical area and an entry point into the hippocampal memory formation (Burwell and Amaral, 1998a, b). We monitored cue responses in the same V1 and POR neurons across many days and imaging sessions, allowing us to assay the stability of cue-evoked responses in trained mice. We reliably observed significant visual cue-evoked responses in the same single neurons across 2–10 sessions (Figure 2G). Neurons in both V1 and POR were reliably driven by the same preferred stimulus across days, and across-day stability was similar across areas (Figure S3B; p=0.188, V1 *vs.* POR, Kruskal-Wallis).

We also quantified how stably POR and V1 populations reflected the salience of the FC in food-restricted mice across sessions, by calculating a response bias index ([response to one cue] / [sum of all cue responses]) for each imaging day, in each field-of-view (FOV). We found that the visually responsive neurons in each FOV in POR, but not in V1, demonstrated a bias to the FC that was reliable across sessions and across mice (Figure 2H). Furthermore, in contrast to a previous study showing changes in the shape of visual response timecourses across days during learning (Makino and Komiyama, 2015), we found that, in well-trained mice, individual V1 and POR neurons showed response timecourses of similar shape across days (Figure S3C; median across-day correlation coefficient >0.95 in both V1 and POR).

Anatomical and functional mapping of lateral amygdala axonal inputs to POR

The lateral amygdala (LA) is important for stimulus-outcome associations and encoding the motivational salience of sensory cues, likely involving a dialogue between neurons in rhinal association cortex and LA/BLA (LeDoux, 2003; Morrison and Salzman, 2010; Paz et al., 2006). Interestingly, in rats and cats, LA neurons project to postrhinal and other lateral visual cortical areas, but not to early visual cortex (Krettek and Price, 1977; Pitkanen et al., 2000). We investigated this connectivity in mice, using both anterograde and retrograde tracing techniques. Retrograde tracing, via injections of CTB-Alexa488 into POR, resulted in labeled somata in the amygdala, mostly confined to LA (Figure S5A). Anterograde tracing using injection of AAV-DIO-synaptophysin-GFP into LA of vGlut2-ires-cre knock-in mice (Vong et al., 2011) labeled glutamatergic axonal boutons in entorhinal, rhinal, and

secondary sensory cortices, but not in primary sensory cortices (Figure 3A). In particular, dense labeling of amygdalo-cortical boutons was present in POR, but not V1. We further characterized feedback axons to POR ($LA^{\rightarrow POR}$) by injecting AAV6-cre (which has pronounced retrograde transport) into POR, and injecting AAV-DIO-ChR2-mCherry into LA (Figure S5B). This projection-specific mapping demonstrated dense collaterals of $LA^{\rightarrow POR}$ projections throughout rhinal cortex, but relatively few collaterals in secondary sensory or entorhinal cortices (Figure S5A). Further, $LA^{\rightarrow POR}$ axons showed high connectivity with POR neurons, as assessed using ChR2-assisted circuit mapping (Figure 3B). Functional, monosynaptic connections from $LA^{\rightarrow POR}$ axons were confirmed in 12/12 layer 2/3 POR pyramidal neurons examined.

Anterograde tracing also revealed direct projections from POR to LA and to BLA (Figure S5C). Together, these data suggest the possibility of a disynaptic excitatory loop in which POR neurons might synapse directly onto $LA^{\rightarrow POR}$ projection neurons. We confirmed this hypothesis using projection-specific, trans-synaptic rabies tracing (Callaway and Luo, 2015). Briefly, we expressed rabies glycoprotein (AAV8-CAG-FLEX-Rabies-G) and TVA-mCherry (AAV8-FLEX-TVA-mCherry) into LA neurons (Figure 3C1 and 3C4, top-left panels). Four weeks later, we injected pseudotyped G-deleted rabies (SAD-ΔG-EnvA-GFP) into POR, leading to rabies infection of TVA+ $LA^{\rightarrow POR}$ axons, trafficking to somata, monosynaptic retrograde transport to afferents of $LA^{\rightarrow POR}$ neurons, and expression of GFP (Figure 3C3). We found GFP+ afferents to $LA^{\rightarrow POR}$ neurons in several subcortical regions that could provide information regarding the motivational relevance of sensory stimuli, including basolateral amygdala, basomedial amygdala, and sensory thalamus (Figure S5D). As hypothesized above, we also found GFP+ afferents to $LA^{\rightarrow POR}$ neurons localized to POR and nearby regions (Figure 3C4), demonstrating that $LA^{\rightarrow POR}$ neurons receive direct input from POR neurons. These anatomical findings reveal that $LA^{\rightarrow POR}$ neurons are part of a reciprocal loop, receiving visual information from POR and sending feedback to POR that may reflect the learned value of the visual cue.

We observed some degree of selectivity in the cortical afferents to $LA^{\rightarrow POR}$, as rabies tracing of inputs to $LA^{\rightarrow POR}$ neurons (Figure 3C1 and 3C2) only labeled neurons in a subset of all cortical areas found to project to any glutamatergic LA neurons (Figure 3D). Furthermore, when we applied projection-specific rabies tracing to LA/BLA projections to lateral entorhinal cortex ($LA^{\rightarrow LEnt}$), we observed that cortical neurons projecting to $LA^{\rightarrow LEnt}$ neurons were located, on average, more ventrally than those projecting to $LA^{\rightarrow POR}$ neurons (Figure 3E). These data show that LA neurons projecting to different dorsal/ventral locations in lateral cortex receive stronger reciprocal input from cortical neurons in the same dorsal/ventral region. These findings regarding the specific afferents and the projection targets of glutamatergic $LA^{\rightarrow POR}$ neurons, and their strong monosynaptic connectivity with pyramidal neurons in POR, suggest that $LA^{\rightarrow POR}$ neurons could relay information to POR regarding the salience of motivationally relevant visual stimuli.

To test this hypothesis, we established methods for chronic calcium imaging of subcortical axonal inputs to cortex – specifically, of $LA^{\rightarrow POR}$ axons – in behaving mice. We expressed GCaMP6f in excitatory neurons in LA, performed a cortical window implant and epifluorescence mapping of POR, followed by two-photon imaging in superficial layers of

POR ($LA^{\rightarrow POR}$ imaging in n=4 mice, n=317 axons, n=3–12 sessions/field-of-view for a total of 33 imaging sessions; Figure 4A–B). In contrast to previous axon imaging studies (Glickfeld et al., 2013; Petreanu et al., 2012), we combined the signal from different boutons confirmed to be from the same axon (Nelson and Mooney, 2016), as signals from these boutons were highly correlated. As with cell bodies in V1 and POR, we observed cue-evoked activity in $LA^{\rightarrow POR}$ axons prior to lick onset and to delivery of Ensure (Figure 4C–E). We found that 13% (42/317) of all active LA axons recorded were driven by visual cues (Figure 4F, pie chart), and that the majority of these axons were only responsive to one visual cue (Figure 4D–E; $p<0.05$; 1 cue: 86%; 2 cues: 12%; 3 cues: 2%; Tukey's HSD). Strikingly, over four times more $LA^{\rightarrow POR}$ axons preferred the FC to the QC or NC (Figure 4F; $p<0.05$; FC: 71%; QC: 12%; NC: 17%; Tukey's HSD). In addition, as in POR, the pooled population cue-evoked response across $LA^{\rightarrow POR}$ axons showed a strong bias to the FC (Figure 4G; FC *vs.* QC: $p<0.001$; FC *vs.* NC: $p<0.001$; QC *vs.* NC: $p>0.05$; Kruskal-Wallis). This population response bias towards the FC emerged within ~400 ms of stimulus onset, well before any licking (Figure S3E–F; FC *vs.* QC: $p=0.01$; FC *vs.* NC: $p=0.01$; QC *vs.* NC: $p=0.99$).

We were able to reliably track the activity of long-range $LA^{\rightarrow POR}$ axons across 2–12 imaging sessions (Figure 4H). $LA^{\rightarrow POR}$ axons were less reliably driven across days than V1 neurons (Figure S3B; V1 *vs.* LA: $p=0.01$; V1 *vs.* POR: $p=0.18$; POR *vs.* LA: $p=0.3$; Kruskal-Wallis). We found that the average FC bias across simultaneously recorded sets of $LA^{\rightarrow POR}$ axons was stable across days, albeit more variable than in POR (compare Figures 4I and 2H). Furthermore, we found that while individual $LA^{\rightarrow POR}$ axons showed response timecourses of similar shape across days (median shape correlation coefficient > 0.9), their responses were less stable across imaging sessions than neurons in V1 or POR (Figure S3C; V1 *vs.* LA: $p<0.001$, POR *vs.* LA: $p=0.004$; Kruskal-Wallis).

POR neurons responded to cues in a manner similar to V1 neurons in some ways, and to $LA^{\rightarrow POR}$ neurons in other ways. As described above, orientation tuning in POR of naïve mice (Figure S2) was qualitatively similar to that previously observed in V1 (Niell and Stryker, 2008). Additionally, response reliability and latency were similar across V1 and POR neurons (Figures S3B–C & S6A), while $LA^{\rightarrow POR}$ neurons generally had longer latencies (though short latency responses were observed in some neurons; Quirk et al., 1995). In contrast, food cue response biases were observed in both POR and $LA^{\rightarrow POR}$, but not V1 of food-restricted, trained mice (Figure 2F & 4G). Finally, in comparing the magnitude of cue-specific biases across all three areas, we found that $LA^{\rightarrow POR}$ axons showed a larger bias to the FC than POR or V1 neurons (Figure 4J; V1 *vs.* LA: $p=0.002$, POR *vs.* LA: $p=0.023$, V1 *vs.* POR: $p=0.24$; Kruskal-Wallis). These data are consistent with a role for $LA^{\rightarrow POR}$ axons in emergent, motivation-specific biasing of visual responses in POR.

State-dependent processing of food cues in POR and $LA^{\rightarrow POR}$ neurons

If the current needs of the mouse indeed determine the relative salience of the food cue, we reasoned that the observed FC response biases should be diminished in a sated state. We compared the responses of V1, POR and $LA^{\rightarrow POR}$ neurons in a food-restricted (FR) state

and a sated state during the same imaging session, prior to and following a 30–75 minute meal in the absence of visual cues, during which mice licked to receive drops of Ensure until they rejected intake (after consuming ~1–4 mL; Figure 5A). In order to compare cue-evoked responses across states, sessions, neurons, and brain areas, we normalized cue-evoked responses of each visually-responsive neuron to the average response during the initial imaging run in each session, in which mice were food-restricted (state-normalized ΔF/F, Figure 5B–C). In all three areas, we observed neurons that significantly modulated their FC response between FR and sated states (Figure 5B–C). In POR and $LA^{\rightarrow POR}$ populations, more neurons showed decreased *vs.* increased activity following satiety, while this was not the case in V1 neurons (Figure 5C, pie chart insets). Further, the average normalized FC response across neurons (thick black lines in Figure 5C) decreased with satiety in POR ($p<0.001$; Wilcoxon Sign-Rank test), and trended towards a decrease in $LA^{\rightarrow POR}$ ($p=0.07$), but not in V1 ($p=0.618$).

In order to compare the effects of satiety on FC responses across areas, we calculated a hunger modulation index for each neuron (positive value: FR response>sated response; negative value: FR response<sated response). We observed significantly positive hunger modulation indices in POR and $LA^{\rightarrow POR}$, but not in V1 (Figure 5D; POR: $p<0.0001$, $LA^{\rightarrow POR}$: $p=0.019$, V1: $p=0.48$; Wilcoxon Sign-Rank test against 0). FC responses showed greater hunger modulation in POR and $LA^{\rightarrow POR}$ than in V1 (Figure 5D; V1 *vs.* POR: $p=0.023$; V1 *vs.* LA: $p=0.0002$; POR *vs.* LA: $p=0.332$; Kruskal-Wallis), while this was not the case for QC or NC responses (Figure 5E; $p>0.05$, Kruskal-Wallis). To control for changes in activity over time during the imaging session, we performed the same protocol, but without providing access to Ensure in the period between food-restricted and "sham-satiation" runs (Figure S1A). During "sham-satiation" sessions, behavioral performance in late runs was remarkably similar to performance in early runs (Figure S1B), which was also reflected in a low response modulation index (comparing early runs with late runs) that was similar in POR, LA, and V1 (Figure 5E; $p>0.05$ for all pairwise comparisons across areas, for all three cues, Kruskal-Wallis).

These findings led us to ask whether the population bias towards food cues, observed in POR and $LA^{\rightarrow POR}$ axons in food-restricted mice (Figures 2F, 4G), was 'hard-wired' in these well-trained mice, or whether the bias was specific to the food-restricted state. Interestingly, while there was a response bias to the FC in POR and $LA^{\rightarrow POR}$ in the sham-satiation condition (POR: FC vs. QC: $p=0.011$, FC vs. NC: $p=0.002$; LA: FC vs. QC: $p=0.027$, FC vs. NC: $p=0.31$; 2-way ANOVA with Tukey *post hoc* test), we found that a FC bias was no longer evident in sated mice (Figure 5G, $p>0.05$ across all areas, 2-way ANOVA). A quantification of bias across areas and states revealed that, similar to human neuroimaging studies, visual response biases were both hunger-state dependent and food cue-specific (Figure 5F–G). Thus, mice exhibited both area-and hunger-dependent biases in the average population response to food cues *vs.* non-food cues.

These data establish that population responses, *when averaged across trials*, show hunger-dependent biases towards food cues, as in bulk neuroimaging studies in humans. We next asked whether the motivational effects observed in our cellular ensemble recordings across dozens of neurons were robust enough to reliably reflect the influence of hunger state at the

more behaviorally-relevant timescale of *single trials* (de Araujo et al., 2006; Pagan et al., 2013). To this end, we considered the ability of an ideal observer to deduce, from consideration of FC responses across the entire sample of simultaneously recorded neurons, whether a given FC trial was recorded during a food-restricted (FR) or a sated state. As a control for possible changes in sensory response adaptation, fatigue, and/or slight changes in the imaging plane sectioning of a given cell across hours, we compared single-trial ensemble decoding of FR *vs.* sated trials with decoding of FR *vs.* sham-satiation trials (Figure 6A–C). Using ensemble responses of POR neurons, we found that a simple linear classifier was twice as accurate at discriminating FR from sated trials as it was at discriminating FR from sham-satiation trials (Figure 6A; 30% *vs.* 15% greater accuracy than chance at 2 seconds post FC onset). Similar effects were observed in $LA^{\rightarrow POR}$ axon ensemble recordings (Figure 6C; 17% *vs.* 6% above chance at 2 seconds post FC onset). By contrast, when ensembles of V1 recordings were used, the classifier also performed above chance, but did not show improved accuracy discriminating FR *vs.* sated trials as compared to FR *vs.* sham-satiation trials (24% *vs.* 18% above chance). While sham-satiation was a useful control for complete satiation, it is nevertheless surprising that sham-satiation was at all distinguishable from the FR state, given the similar behavioral performance in these two states (Figure S1B). This finding could be due to partial satiation from consumption of Ensure earned during earlier task performance (mice performing the Go/NoGo task during the sham-satiation condition have received ~0.6 mL of Ensure during the initial FR run). These data also revealed information regarding hunger state was already present in POR and $LA^{\rightarrow POR}$ ensemble responses as early as 200 ms after the FC onset (Figure 6B–C).

Taken together, these analyses of ensemble activity suggests that information about hunger state might be present at the population level even within V1, but that POR and $LA^{\rightarrow POR}$ ensembles are relatively more sensitive to changes in hunger state, consistent with distinct afferent inputs to these areas. By contrast, when a similar analysis was used to distinguish which among two non-rewarded visual cues (QC or NC) was presented on a given trial, the linear classifier accuracy was high in both V1 and POR (Figure 6D; V1: 34% above chance; POR: 34% above chance), but was at chance levels using data across $LA^{\rightarrow POR}$ axons (likely due to the paucity of $LA^{\rightarrow POR}$ axons responding to the QC or the NC, Figure 4F).

Trial-to-trial variability and the effects of trial history

One factor that can affect population decoding across areas is trial-to-trial response variability, potentially reflecting non-sensory influences on sensory responses (Nienborg et al., 2012). To investigate trial-to-trial variability of neurons, we calculated the Fano factor (trial-to-trial variance divided by mean response). $LA^{\rightarrow POR}$ axons (Figure 7A) showed significantly higher trial-to-trial variability than POR neurons (Figure 7A), which in turn showed significantly higher variability than V1 neurons (Figure 7A; V1 *vs.* POR: $p<0.001$; V1 *vs.* LA: $p<0.001$; POR *vs.* LA: $p<0.001$; Kruskal-Wallis). Previous studies showed a similar increase in trial-to-trial response variability from retina to visual thalamus to V1 (Kara et al., 2000).

We hypothesized that the high trial-to-trial variability of responses in POR and $LA^{\rightarrow POR}$ neurons may be partially explained by trial history, specifically, whether a FC stimulus was

preceded by another FC (>85% of FCs led to reward delivery in FR mice) or by a QC or NC. For all FC-preferring cells in all areas, we assayed how the magnitude of a FC response differed when preceded by a FC, *vs.* by one or more non-FCs ($R_{FC\rightarrow FC}$ & $R_{nonFC\rightarrow FC}$ respectively; 'R_{FC}': FC response; Figure 7B). We found individual example neurons for which the FC response was more than *two-fold* larger in those trials preceded by non-FCs than by a FC (Figure 7B) – a level of modulation on par with effects of manipulating hunger state. We quantified how previous trial history modulated FC responses across areas, using a trial history modulation index (positive value: $R_{nonFC\rightarrow FC} > R_{FC\rightarrow FC}$, negative value: $R_{nonFC\rightarrow FC} < R_{FC\rightarrow FC}$). In all three areas, we found neurons that were significantly modulated by previous trial history, as compared to shuffled controls (Figure 7C; V1: 10%; POR: 26%; LA: 23%). Cumulative distributions of trial history modulation index magnitudes across neurons in each area revealed that V1 neurons were substantially less affected by trial history than POR and $LA^{\rightarrow POR}$ neurons (Figure 7D; V1 *vs.* POR: p=0.03; V1 *vs.* LA: p<0.001; POR *vs.* LA: p=0.39; Kruskal-Wallis; median magnitude of modulation: V1: 0.31; POR: 0.69; $LA^{\rightarrow POR}$: 1.28). Behavioral responses were also modulated by trial history, with longer median latency to onset of first lick on FC trials preceded by non-FC trials than by FC trials (1.86 s *vs.* 1.74 s, p<0.001, paired t-test).

Non-visual, task-modulated activity across areas

Our data suggest that POR neurons contain information regarding the identity and value of cues. We next asked whether delivery of the reward is also represented in the activity of V1, POR, and $LA^{\rightarrow POR}$ neurons. To isolate non-visually evoked, task-related responses, we exploited the trial-to-trial variability in the onset of lick responses to train a general linear model (GLM; Hartmann et al., 2011; Pinto and Dan, 2015) to estimate lick-, reward- and false alarm-related changes in neuronal activity. In all areas, we found examples of non-visually-responsive cells that increased their activity only at the time of Ensure delivery (Figure 8A, $LA^{\rightarrow POR}$ axon) or at the onset of licking (Figure 8B, V1 cell body). Because we designed our experiments to guarantee (i) accurate and consistent behavioral performance, (ii) delayed reaction times, and (iii) immediate lick-triggered Ensure delivery during the reward window (Figure 1D), we could not definitively ascribe task-related responses of neurons to licking *vs.* lick-induced outcomes. Thus, we classified task related neurons as belonging to one of three categories: 'Lick-reward', 'Lick-false alarm', and 'Lick-motor' (Figure S7A–C). We found that a larger fraction of $LA^{\rightarrow POR}$ axons were categorized as Lick-reward as compared to POR or V1 neurons (Figure 7D, p<0.05, Tukey's HSD; see also Figure S7D). This demonstrates that $LA^{\rightarrow POR}$ feedback axons contain information about food reward delivery in addition to information about the motivational salience of food cues (Namburi et al., 2015).

We also observed a subset of neurons in each area that were significantly *suppressed* by presentation of visual cues. Previous studies have shown that spontaneous firing rates in awake rodent visual cortex and LA are low (0.1–1 Hz; Niell and Stryker, 2008; Sangha et al., 2013). To reduce the contribution of floor effects (i.e. lack of pre-cue activity) in the evaluation of significant cue-induced suppression, we only evaluated those cells with high and variable pre-stimulus activity (Figure S8A–B). Unlike visually excited neurons, most visually suppressed neurons responded to all three visual cues, similar to 'suppressed-by-

contrast' cells frequently described in retina (Figure S8C; Mastronarde, 1985), thalamus (Piscopo et al., 2013), and V1 (Niell and Stryker, 2008). Further, this small sample of neurons did not appear to demonstrate pronounced biases to the FC, or hunger-dependent FC response modulation (Figure S8E–F).

Discussion

Using chronic two-photon calcium imaging of populations of layer 2/3 cortical neurons, we found a visual response bias to motivationally salient learned food cues in postrhinal cortex (POR), but not in V1. Strikingly, this food cue bias was abolished by satiation. Using a combination of circuit mapping techniques, we identified reciprocal monosynaptic connectivity between POR neurons and glutamatergic feedback projections to POR from lateral amygdala ($LA^{\rightarrow POR}$), an area implicated in updating the value of sensory cues. Long-term recordings of activity in visually-driven $LA^{\rightarrow POR}$ axons revealed hunger-dependent food cue biases that were larger than in POR or V1. Further, the recent history of rewards and reward-predicting cues had an increasingly strong impact on food cue responses in V1, POR, and $LA^{\rightarrow POR}$ neurons. Our findings of cue-, state-, and brain area-dependent enhancement of neuronal responses to salient food cues in a genetically-accessible model system set the stage for chronic physiological recordings and pathway-specific silencing experiments that should enrich our understanding of subcortical inputs in guiding selective cortical processing of motivationally relevant cues.

Activity in postrhinal cortex reflects both stimulus identity and value

POR in rodents has received little attention, and its response properties have not been previously characterized using cellular imaging. Our anatomical connectivity findings (Figure 3) and others studies (Burwell and Amaral, 1998a; Wang et al., 2012) suggest that POR plays a key role as a gateway between many well-studied neural networks, including the hippocampal formation, early visual cortex, and the amygdala. As such, POR is likely to reflect and integrate aspects of each network. For example, POR likely serves as a relay of visual object information to hippocampus, as lesion studies have implicated POR in object recognition, object learning, and object-directed orienting (Bussey et al., 2003; Davies et al., 2007; Gastelum et al., 2012). The few physiology studies that have recorded from identified POR (Burwell and Hafeman, 2003; Furtak et al., 2012) or nearby lateral cortical areas in rats (Vermaercke et al., 2014) are consistent with this notion. For example, LFP recordings during a visual object discrimination task show that POR activity contains information regarding both object identity and location (Furtak et al., 2012).

We found that POR also demonstrated several features of visual cortical areas such as retinotopic organization (which allowed reliable recordings from precisely the same area across mice). We found reliable, short-latency visual responses in POR neurons in naïve, awake mice (Figure S2) that were often sharply tuned to stimulus orientation, consistent with direct input from early visual areas (Wang and Burkhalter, 2007; Wang et al., 2012) which contain sharply orientation-tuned neurons (Niell and Stryker, 2008).

In addition, consistent with previous findings in primate rhinal cortex (Liu et al., 2000), our data also demonstrate that POR neurons encode stimulus value, given their hunger-

dependent bias towards food cues and sensitivity to trial history. It is possible that these effects could arise from inputs from early sensory cortical neurons, which can reflect aspects of stimulus value and reward (Fritz et al., 2003; Komiyama et al., 2010). For example, studies of V1 have shown evidence of response changes with learning (Makino and Komiyama, 2015; Poort et al., 2015) and the presence of reward timing (Shuler and Bear, 2006). We observed that while trial history had a weak influence on a subset of V1 neurons, effects in POR were more pronounced. Furthermore, using a linear classifier to analyze ensemble neuronal activity in single trials, we identified differences in population coding across food-restricted and sated states in V1, but here, again, the influence of state was greater in POR than V1. These data suggest that hunger state information may be more linearly separable in rhinal cortex than in earlier visual cortex (Pagan et al., 2013). It will be important, in future studies, to specifically silence sensory and/or reward-related inputs to POR in order to characterize how POR integrates information about stimulus identity and stimulus value. Similarly, investigation of POR projections to other visual areas could provide insights on the role of feedback in value-based responses in early visual cortex.

The POR response bias we observed towards a motivationally-salient learned visual food cue was not present in POR of naïve mice, or in trained mice in the sated state (Figure S2D). Because average population responses in V1 did not exhibit the same bias, or sensitivity to hunger state, our findings in POR are unlikely to be explained by ‘bottom-up’ inputs (Figure 2) or cortex-wide neuromodulatory inputs related to global arousal. Instead, we suggest that the FC bias may be due to a learned, state-dependent source of top-down feedback that is engaged following learning (Atiani et al., 2014; Makino and Komiyama, 2015). While elements of this circuit may generalize to other cortical areas and modalities, the direct inputs to POR from LA and other subcortical brain regions make POR a natural locus for integration of information regarding stimulus identity and value. Future studies could reverse cue outcome associations to dissociate the neural representations of stimulus identity and value.

Amygdalo-cortical projections relay information about state-dependent object salience

We identified a spatially localized, disynaptic reciprocal excitatory loop between POR and LA, based on monosynaptic rabies tracing, together with other circuit mapping techniques. This provides an anatomical substrate by which POR (and other rhinal and entorhinal areas) might ‘ping’ (Klavir et al., 2013) specific subsets of LA neurons regarding object identity or location, and receive rapid feedback regarding state-dependent object value from these same LA neurons. Indeed, as compared to POR neurons, our recordings of $LA^{\rightarrow POR}$ axons yielded responses that were even more selective to food cues, and more strongly modulated by hunger state and trial history. These data suggest that $LA^{\rightarrow POR}$ axons represent a source of information regarding the instantaneous motivational value of sensory cues. Activity of LA and BLA neurons have been suggested to selectively facilitate feedforward information flow, such as from rhinal to entorhinal cortex (LEnt; Paz et al., 2006). As it is difficult to disentangle reciprocal loops using anatomical methods alone, future cellular imaging studies incorporating retrograde labeling in LA could test whether $POR^{\rightarrow LA/BLA}$ and $POR^{\rightarrow LEnt}$ projection neurons are more sensitive to hunger state and trial history than, for example, $POR^{\rightarrow V1}$ neurons (Wang et al., 2011). More generally, anatomical loops between LA/BLA

and cortical targets such as anterior cingulate cortex (Klavir et al., 2013), prelimbic, and infralimbic cortex (Little and Carter, 2013) may also reveal similar reciprocal disynaptic connectivity and function.

Many studies have demonstrated a role for the LA/BLA in learning the value of visual stimuli (Morrison and Salzman, 2010), and the importance of direct LA/BLA projections to cortex in learning cue-outcome associations (Sparta et al., 2014). While we did not directly investigate the circuit mechanisms by which POR develops a biased representation of specific cues during learning, it is possible that the LA feedback to POR is important during this process. An intact amygdala is essential for updating the value of cues following changes in external cue-reward associations (Morrison and Salzman, 2010). By contrast, our experiments show that, in situations where the cue-reward association is fixed, LA is likely involved in continuous adjustment of the effective value of specific learned cues based on factors such as hunger state, similar to the known role of BLA in reinforcer devaluation via selective satiation with a particular reward (Johnson et al., 2009). Indeed, several studies of the functional connectivity between BLA and more anterior (gustatory) temporal cortex suggest a key role for BLA in relaying value information to cortical representations of tastants and learned, taste-predicting auditory cues in water-restricted rats (Fontanini et al., 2009; Samuelsen et al., 2012). The effects of motivational state on $LA^{\rightarrow POR}$ activity may arise from inputs from a variety of areas, including BLA neurons (Figure S5D) and ventral tegmental area dopaminergic neurons, which are themselves sensitive to hunger state (Aitken et al., 2015) and trial history (Hamid et al., 2016).

A mouse model for motivation-dependent processing of relevant sensory cues

A large number of human fMRI studies found enhanced neural processing of food cues in hungry *vs.* sated states in temporal lobe areas and amygdala, but not visual cortex. Further, as compared to healthy subjects, individuals with eating disorders, obesity, or elevated propensity for weight gain showed less of a drop in food cue responses in sated *vs.* hungry states (Huerta et al., 2014; Sun et al., 2015). These studies report average activity across many neurons. By contrast, the technical challenges in single-neuron electrophysiological recordings across slowly changing motivational states and across sessions in animal models have impeded our understanding of the circuits that underlie this form of motivation-dependent sensory processing. Long-term two-photon calcium imaging of populations of neurons in behaving mice provides a platform for monitoring the sensory and cognitive effects of slow changes in motivation, with high yield and single-trial sensitivity. Strikingly, when averaged across neurons within each area, our data are consistent with human neuroimaging studies, which consistently report hunger-dependent food cue biases in association cortex, but not in V1. Nevertheless, we find that responses of a small subset of individual neurons in V1 can be modulated up or down by hunger state, and that information about hunger state does exist at the level of ensembles of V1 neurons. While we focused on the effects of hunger and satiety on neuronal responses to food cues, the circuit described here could exhibit response biases to relevant cues across a host of other motivational drive states. Thus, our work provides a much-needed bridge (Badre et al., 2015) between the many basic and clinical studies of visual food cue processing in humans, and a similar paradigm that provides cellular resolution in a genetically-accessible model organism.

In conclusion, our findings suggest that individual mouse POR and LA neurons integrate information about stimulus identity and hunger state. In the future, our paradigm could be expanded to investigate selective processing across multiple motivations. For example, responses from the *same* POR and LA neurons to both food and water cues could be tracked across sessions during food or water restriction, and during artificial induction of hunger- and thirst-like states via optogenetic manipulations of discrete hypothalamic populations (Aponte et al., 2011; Oka et al., 2015). Manipulating multiple motivational states during chronic monitoring of identified cortical neurons and subcortical inputs to cortex in a genetically accessible model system should enable the dissection of motivation-specific selective attention and the circuits that underlie this phenomenon.

Experimental Procedures

All animal care and experimental procedures were approved by the Beth Israel Deaconess Medical Center Institutional Animal Care and Use Committee. Animals were housed with standard mouse chow and water provided *ad libitum*, unless specified otherwise. Mice used for *in vivo* two-photon imaging (n=15 male C57BL/6 mice, n=4 male EMX-cre mice, age at surgery: 9–15 weeks) were instrumented with a headpost and a 3 mm cranial window, centered over either primary visual cortex or lateral cortex including postrhinal cortex. For additional details, see Supplemental Experimental Procedures.

Supplementary Material

Refer to Web version on PubMed Central for supplementary material.

Acknowledgments

We would like to thank R. Fallon, A. Bouck, S. Subramanian, N. Patel, A. Peck, M. Gyetvan, G. Niyazov, S. Wang, and G. He for help with training mice and analyzing anatomy data as well as G. Goldey for developing lateral cranial window surgeries. We would also like to thank R. Johnson, Drs. Born, Harvey, Buckner, and Hartmann for helpful discussion. We thank Drs. Jayaraman, Kerr, Kim, Looger, and Svoboda and the GENIE Project at Janelia Farm Research Campus, Howard Hughes Medical Institute for use of GCaMP6. Support was provided by a Davis Family Foundation Postdoctoral Fellowship (CRB), NIH F31 105678 (RNR), NIH T32 5T32DK007516 (AUS), NIH R01 DK075632, R01 DK096010, R01 DK089044, P30 DK046200, and P30 DK057521 (BBL), and an NIH Director's New Innovator Award DP2DK105570, NIH R01 DK109930, and grants from the Smith Family Foundation, Klarman Family Foundation, McKnight Foundation, American Federation for Aging Research, the Pew Scholars Program in the Biomedical Sciences, and the Boston Nutrition and Obesity Research Center (MLA).

References

Aitken TJ, Greenfield VY, Wassum KM. Nucleus accumbens core dopamine signaling tracks the need-based motivational value of food-paired cues. J Neurochem. 2015

Andermann ML, Kerlin AM, Roumis DK, Glickfeld LL, Reid RC. Functional specialization of mouse higher visual cortical areas. Neuron. 2011; 72:1025–1039. [PubMed: 22196337]

Aponte Y, Atasoy D, Sternson SM. AGRP neurons are sufficient to orchestrate feeding behavior rapidly and without training. Nat Neurosci. 2011; 14:351–355. [PubMed: 21209617]

Atiani S, David SV, Elgueda D, Locastro M, Radtke-Schuller S, Shamma SA, Fritz JB. Emergent selectivity for task-relevant stimuli in higher-order auditory cortex. Neuron. 2014; 82:486–499. [PubMed: 24742467]

Badre D, Frank MJ, Moore CI. Interactionist Neuroscience. Neuron. 2015; 88:855–860. [PubMed: 26637794]

Baxter MG, Murray EA. The amygdala and reward. Nat Rev Neurosci. 2002; 3:563–573. [PubMed: 12094212]

Beaudin SA, Singh T, Agster KL, Burwell RD. Borders and comparative cytoarchitecture of the perirhinal and postrhinal cortices in an F1 hybrid mouse. Cereb Cortex. 2013; 23:460–476. [PubMed: 22368084]

Blair HT, Sotres-Bayon F, Moita MA, Ledoux JE. The lateral amygdala processes the value of conditioned and unconditioned aversive stimuli. Neuroscience. 2005; 133:561–569. [PubMed: 15878802]

Burwell RD, Amaral DG. Cortical afferents of the perirhinal, postrhinal, and entorhinal cortices of the rat. J Comp Neurol. 1998a; 398:179–205. [PubMed: 9700566]

Burwell RD, Amaral DG. Perirhinal and postrhinal cortices of the rat: interconnectivity and connections with the entorhinal cortex. J Comp Neurol. 1998b; 391:293–321. [PubMed: 9492202]

Burwell RD, Hafeman DM. Positional firing properties of postrhinal cortex neurons. Neuroscience. 2003; 119:577–588. [PubMed: 12770570]

Bussey TJ, Saksida LM, Murray EA. Impairments in visual discrimination after perirhinal cortex lesions: testing 'declarative' vs. 'perceptual-mnemonic' views of perirhinal cortex function. Eur J Neurosci. 2003; 17:649–660. [PubMed: 12581183]

Callaway EM, Luo L. Monosynaptic Circuit Tracing with Glycoprotein-Deleted Rabies Viruses. J Neurosci. 2015; 35:8979–8985. [PubMed: 26085623]

Chen JL, Margolis DJ, Stankov A, Sumanovski LT, Schneider BL, Helmchen F. Pathway-specific reorganization of projection neurons in somatosensory cortex during learning. Nat Neurosci. 2015; 18:1101–1108. [PubMed: 26098757]

Chen TW, Wardill TJ, Sun Y, Pulver SR, Renninger SL, Baohan A, Schreiter ER, Kerr RA, Orger MB, Jayaraman V, et al. Ultrasensitive fluorescent proteins for imaging neuronal activity. Nature. 2013; 499:295–300. [PubMed: 23868258]

Cornier MA, McFadden KL, Thomas EA, Bechtell JL, Eichman LS, Bessesen DH, Tregellas JR. Differences in the neuronal response to food in obesity-resistant as compared to obesity-prone individuals. Physiol Behav. 2013; 110–111:122–128.

Cornier MA, Von Kaenel SS, Bessesen DH, Tregellas JR. Effects of overfeeding on the neuronal response to visual food cues. Am J Clin Nutr. 2007; 86:965–971. [PubMed: 17921372]

Davies M, Machin PE, Sanderson DJ, Pearce JM, Aggleton JP. Neurotoxic lesions of the rat perirhinal and postrhinal cortices and their impact on biconditional visual discrimination tasks. Behav Brain Res. 2007; 176:274–283. [PubMed: 17092577]

de Araujo IE, Gutierrez R, Oliveira-Maia AJ, Pereira A Jr, Nicolelis MA, Simon SA. Neural ensemble coding of satiety states. Neuron. 2006; 51:483–494. [PubMed: 16908413]

Fontanini A, Grossman SE, Figueroa JA, Katz DB. Distinct subtypes of basolateral amygdala taste neurons reflect palatability and reward. J Neurosci. 2009; 29:2486–2495. [PubMed: 19244523]

Fritz J, Shamma S, Elhilali M, Klein D. Rapid task-related plasticity of spectrotemporal receptive fields in primary auditory cortex. Nat Neurosci. 2003; 6:1216–1223. [PubMed: 14583754]

Furtak SC, Ahmed OJ, Burwell RD. Single neuron activity and theta modulation in postrhinal cortex during visual object discrimination. Neuron. 2012; 76:976–988. [PubMed: 23217745]

Garrett ME, Nauhaus I, Marshel JH, Callaway EM. Topography and areal organization of mouse visual cortex. J Neurosci. 2014; 34:12587–12600. [PubMed: 25209296]

Gastelum ED, Guilhardi P, Burwell RD. The effects of combined perirhinal and postrhinal damage on complex discrimination tasks. Hippocampus. 2012; 22:2059–2067. [PubMed: 22987682]

Glickfeld LL, Andermann ML, Bonin V, Reid RC. Cortico-cortical projections in mouse visual cortex are functionally target specific. Nat Neurosci. 2013; 16:219–226. [PubMed: 23292681]

Hamid AA, Pettibone JR, Mabrouk OS, Hetrick VL, Schmidt R, Vander Weele CM, Kennedy RT, Aragona BJ, Berke JD. Mesolimbic dopamine signals the value of work. Nat Neurosci. 2016; 19:117–126. [PubMed: 26595651]

Hartmann TS, Bremmer F, Albright TD, Krekelberg B. Receptive field positions in area MT during slow eye movements. J Neurosci. 2011; 31:10437–10444. [PubMed: 21775589]

Hatfield T, Han JS, Conley M, Gallagher M, Holland P. Neurotoxic lesions of basolateral, but not central, amygdala interfere with Pavlovian second-order conditioning and reinforcer devaluation effects. J Neurosci. 1996; 16:5256–5265. [PubMed: 8756453]

Higgs S, Rutters F, Thomas JM, Naish K, Humphreys GW. Top down modulation of attention to food cues via working memory. Appetite. 2012; 59:71–75. [PubMed: 22450523]

Holland PC, Gallagher M. Double dissociation of the effects of lesions of basolateral and central amygdala on conditioned stimulus-potentiated feeding and Pavlovian-instrumental transfer. Eur J Neurosci. 2003; 17:1680–1694. [PubMed: 12752386]

Huerta CI, Sarkar PR, Duong TQ, Laird AR, Fox PT. Neural bases of food perception: coordinate-based meta-analyses of neuroimaging studies in multiple modalities. Obesity (Silver Spring). 2014; 22:1439–1446. [PubMed: 24174404]

Jenison RL, Rangel A, Oya H, Kawasaki H, Howard MA. Value encoding in single neurons in the human amygdala during decision making. J Neurosci. 2011; 31:331–338. [PubMed: 21209219]

Johnson AW, Gallagher M, Holland PC. The basolateral amygdala is critical to the expression of pavlovian and instrumental outcome-specific reinforcer devaluation effects. J Neurosci. 2009; 29:696–704. [PubMed: 19158296]

Kara P, Reinagel P, Reid RC. Low response variability in simultaneously recorded retinal, thalamic, and cortical neurons. Neuron. 2000; 27:635–646. [PubMed: 11055444]

Klavir O, Genud-Gabai R, Paz R. Functional connectivity between amygdala and cingulate cortex for adaptive aversive learning. Neuron. 2013; 80:1290–1300. [PubMed: 24314732]

Komiyama T, Sato TR, O'Connor DH, Zhang YX, Huber D, Hooks BM, Gabitto M, Svoboda K. Learning-related fine-scale specificity imaged in motor cortex circuits of behaving mice. Nature. 2010; 464:1182–1186. [PubMed: 20376005]

Krettek JE, Price JL. Projections from the amygdaloid complex to the cerebral cortex and thalamus in the rat and cat. J Comp Neurol. 1977; 172:687–722. [PubMed: 838895]

LaBar KS, Gitelman DR, Parrish TB, Kim YH, Nobre AC, Mesulam MM. Hunger selectively modulates corticolimbic activation to food stimuli in humans. Behav Neurosci. 2001; 115:493–500. [PubMed: 11345973]

LeDoux J. The emotional brain, fear, and the amygdala. Cell Mol Neurobiol. 2003; 23:727–738. [PubMed: 14514027]

Little JP, Carter AG. Synaptic mechanisms underlying strong reciprocal connectivity between the medial prefrontal cortex and basolateral amygdala. J Neurosci. 2013; 33:15333–15342. [PubMed: 24068800]

Liu Z, Murray EA, Richmond BJ. Learning motivational significance of visual cues for reward schedules requires rhinal cortex. Nat Neurosci. 2000; 3:1307–1315. [PubMed: 11100152]

Makino H, Komiyama T. Learning enhances the relative impact of top-down processing in the visual cortex. Nat Neurosci. 2015; 18:1116–1122. [PubMed: 26167904]

Mank M, Santos AF, Direnberger S, Mrsic-Flogel TD, Hofer SB, Stein V, Hendel T, Reiff DF, Levelt C, Borst A, et al. A genetically encoded calcium indicator for chronic in vivo two-photon imaging. Nat Methods. 2008; 5:805–811. [PubMed: 19160515]

Mastronarde DN. Two types of cat retinal ganglion cells that are suppressed by contrast. Vision Res. 1985; 25:1195–1196. [PubMed: 4071998]

Morrison SE, Salzman CD. Re-valuing the amygdala. Curr Opin Neurobiol. 2010; 20:221–230. [PubMed: 20299204]

Namburi P, Beyeler A, Yorozu S, Calhoon GG, Halbert SA, Wichmann R, Holden SS, Mertens KL, Anahtar M, Felix-Ortiz AC, et al. A circuit mechanism for differentiating positive and negative associations. Nature. 2015; 520:675–678. [PubMed: 25925480]

Nelson A, Mooney R. The Basal Forebrain and Motor Cortex Provide Convergent yet Distinct Movement-Related Inputs to the Auditory Cortex. Neuron. 2016; 90:635–648. [PubMed: 27112494]

Niell CM, Stryker MP. Highly selective receptive fields in mouse visual cortex. J Neurosci. 2008; 28:7520–7536. [PubMed: 18650330]

Nienborg H, Cohen MR, Cumming BG. Decision-related activity in sensory neurons: correlations among neurons and with behavior. Annu Rev Neurosci. 2012; 35:463–483. [PubMed: 22483043]

Oka Y, Ye M, Zuker CS. Thirst driving and suppressing signals encoded by distinct neural populations in the brain. Nature. 2015; 520:349–352. [PubMed: 25624099]

Pagan M, Urban LS, Wohl MP, Rust NC. Signals in inferotemporal and perirhinal cortex suggest an untangling of visual target information. Nat Neurosci. 2013; 16:1132–1139. [PubMed: 23792943]

Paton JJ, Belova MA, Morrison SE, Salzman CD. The primate amygdala represents the positive and negative value of visual stimuli during learning. Nature. 2006; 439:865–870. [PubMed: 16482160]

Paz R, Pelletier JG, Bauer EP, Pare D. Emotional enhancement of memory via amygdala-driven facilitation of rhinal interactions. Nat Neurosci. 2006; 9:1321–1329. [PubMed: 16964249]

Petreanu L, Gutnisky DA, Huber D, Xu NL, O'Connor DH, Tian L, Looger L, Svoboda K. Activity in motor-sensory projections reveals distributed coding in somatosensation. Nature. 2012; 489:299–303. [PubMed: 22922646]

Pinto L, Dan Y. Cell-Type-Specific Activity in Prefrontal Cortex during Goal-Directed Behavior. Neuron. 2015; 87:437–450. [PubMed: 26143660]

Piscopo DM, El-Danaf RN, Huberman AD, Niell CM. Diverse visual features encoded in mouse lateral geniculate nucleus. J Neurosci. 2013; 33:4642–4656. [PubMed: 23486939]

Pitkanen A, Pikkarainen M, Nurminen N, Ylinen A. Reciprocal connections between the amygdala and the hippocampal formation, perirhinal cortex, and postrhinal cortex in rat. A review. Ann N Y Acad Sci. 2000; 911:369–391. [PubMed: 10911886]

Poort J, Khan AG, Pachitariu M, Nemri A, Orsolic I, Krupic J, Bauza M, Sahani M, Keller GB, Mrsic-Flogel TD, Hofer SB. Learning Enhances Sensory and Multiple Non-sensory Representations in Primary Visual Cortex. Neuron. 2015; 86:1478–1490. [PubMed: 26051421]

Posner MI. Orienting of attention. Q J Exp Psychol. 1980; 32:3–25. [PubMed: 7367577]

Quirk GJ, Repa C, LeDoux JE. Fear conditioning enhances short-latency auditory responses of lateral amygdala neurons: parallel recordings in the freely behaving rat. Neuron. 1995; 15:1029–1039. [PubMed: 7576647]

Roth MM, Helmchen F, Kampa BM. Distinct functional properties of primary and posteromedial visual area of mouse neocortex. J Neurosci. 2012; 32:9716–9726. [PubMed: 22787057]

Samuelsen CL, Gardner MP, Fontanini A. Effects of cue-triggered expectation on cortical processing of taste. Neuron. 2012; 74:410–422. [PubMed: 22542192]

Sangha S, Chadick JZ, Janak PH. Safety encoding in the basal amygdala. J Neurosci. 2013; 33:3744–3751. [PubMed: 23447586]

Shuler MG, Bear MF. Reward timing in the primary visual cortex. Science. 2006; 311:1606–1609. [PubMed: 16543459]

Sparta DR, Smithuis J, Stamatakis AM, Jennings JH, Kantak PA, Ung RL, Stuber GD. Inhibition of projections from the basolateral amygdala to the entorhinal cortex disrupts the acquisition of contextual fear. Front Behav Neurosci. 2014; 8:129. [PubMed: 24834031]

Sun X, Kroemer NB, Veldhuizen MG, Babbs AE, de Araujo IE, Gitelman DR, Sherwin RS, Sinha R, Small DM. Basolateral amygdala response to food cues in the absence of hunger is associated with weight gain susceptibility. J Neurosci. 2015; 35:7964–7976. [PubMed: 25995480]

Vermaercke B, Gerich FJ, Ytebrouck E, Arckens L, Op de Beeck HP, Van den Bergh G. Functional specialization in rat occipital and temporal visual cortex. J Neurophysiol. 2014; 112:1963–1983. [PubMed: 24990566]

Vong L, Ye C, Yang Z, Choi B, Chua S Jr, Lowell BB. Leptin action on GABAergic neurons prevents obesity and reduces inhibitory tone to POMC neurons. Neuron. 2011; 71:142–154. [PubMed: 21745644]

Wang Q, Burkhalter A. Area map of mouse visual cortex. J Comp Neurol. 2007; 502:339–357. [PubMed: 17366604]

Wang Q, Gao E, Burkhalter A. Gateways of ventral and dorsal streams in mouse visual cortex. J Neurosci. 2011; 31:1905–1918. [PubMed: 21289200]

Wang Q, Sporns O, Burkhalter A. Network analysis of corticocortical connections reveals ventral and dorsal processing streams in mouse visual cortex. J Neurosci. 2012; 32:4386–4399. [PubMed: 22457489]

Yokum S, Ng J, Stice E. Attentional bias to food images associated with elevated weight and future weight gain: an fMRI study. Obesity (Silver Spring). 2011; 19:1775–1783. [PubMed: 21681221]

Ziv Y, Burns LD, Cocker ED, Hamel EO, Ghosh KK, Kitch LJ, El Gamal A, Schnitzer MJ. Long-term dynamics of CA1 hippocampal place codes. Nat Neurosci. 2013; 16:264–266. [PubMed: 23396101]

Highlights

- POR and LA neurons show specific reciprocal connectivity
- POR and LA, but not V1, show a bias to food cues in food-restricted mice
- Satiety abolishes the bias to visual food cues in POR and LA
- Trial-to-trial variability, and effects of trial history, increase from V1 to POR and LA

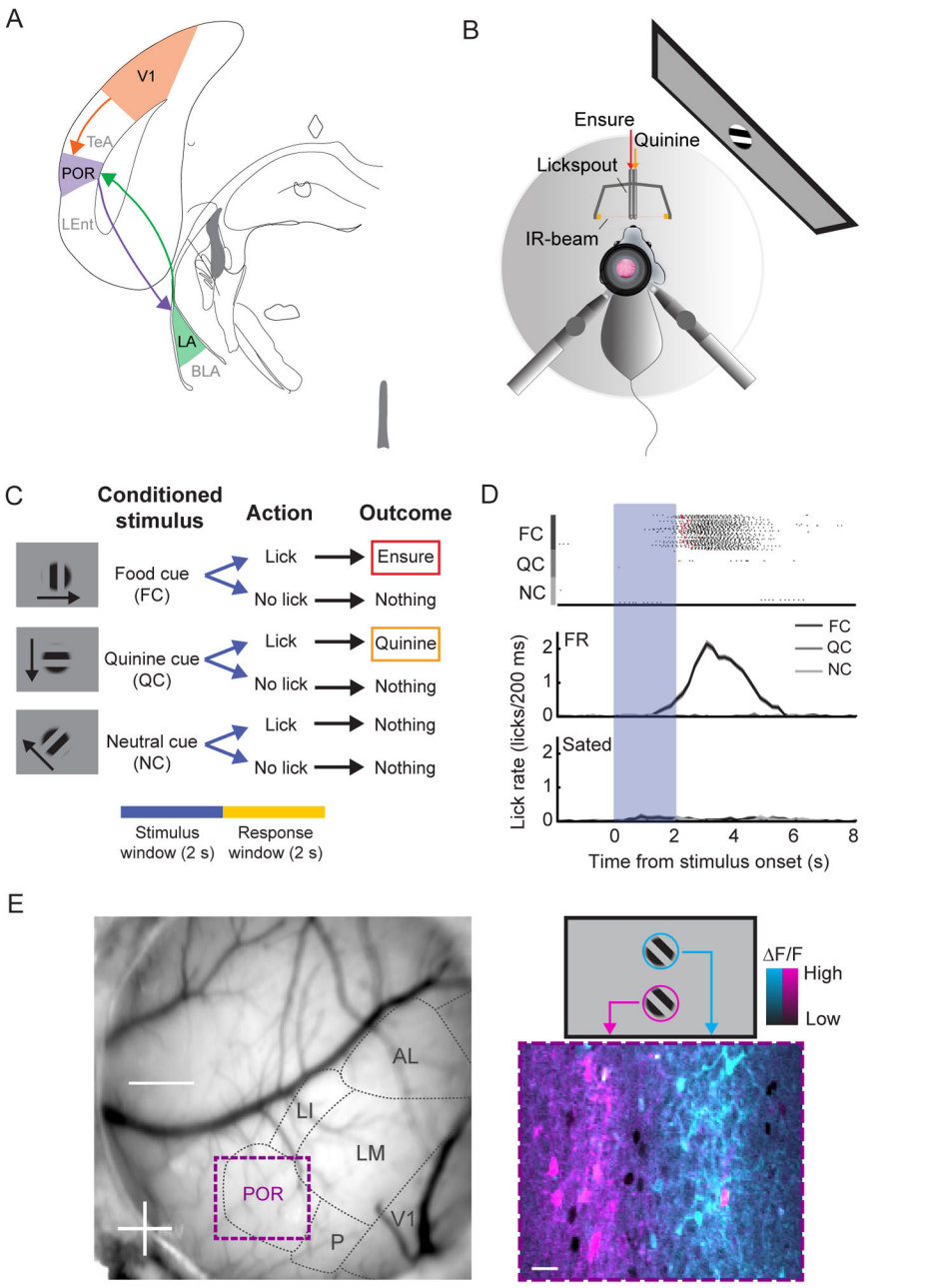

Figure 1. ***In vivo*** **two-photon imaging of head-fixed mice during a Go/NoGo visual discrimination task**

A. Schematic of a V1 - POR - LA circuit.

B. Schematic of setup for *in vivo* two-photon imaging in a mouse performing a Go/NoGo visual discrimination task. Licking is tracked via an IR beam positioned in front of the mouse. Ensure and quinine are delivered via adjacent lickspouts.

C. The task consists of three square-wave gratings drifting in different directions. The cues are presented for 2 s, followed by a 2 s response window. If mice respond with a lick following offset of (i) the food cue (FC), they receive Ensure, (ii) the quinine cue (QC), they receive quinine, and (iii) the neutral cue (NC), they receive nothing.

D. Mice learned to lick following the FC but not following the NC or QC (top: individual licks denoted in black, Ensure delivery in red, quinine delivery in orange). Food-restricted mice performed at a high level. Following satiation, mice refrained from licking and received far fewer food rewards.

E. *Left*: Image of the mouse brain through a cranial window with visual areas demarcated based on intrinsic autofluorescence signal retinotopic mapping, which guided the injection of AAV-GCaMP6f into either V1 or POR. Further retinotopic mapping was done using two-photon calcium imaging of GCaMP6 responses. *Bottom right*: pseudocolor image of average cellular responses (ΔF/F) to stimuli presented either at the top (blue) or bottom (pink) of the screen (see also schematic, *top right*). See also Figure S1.

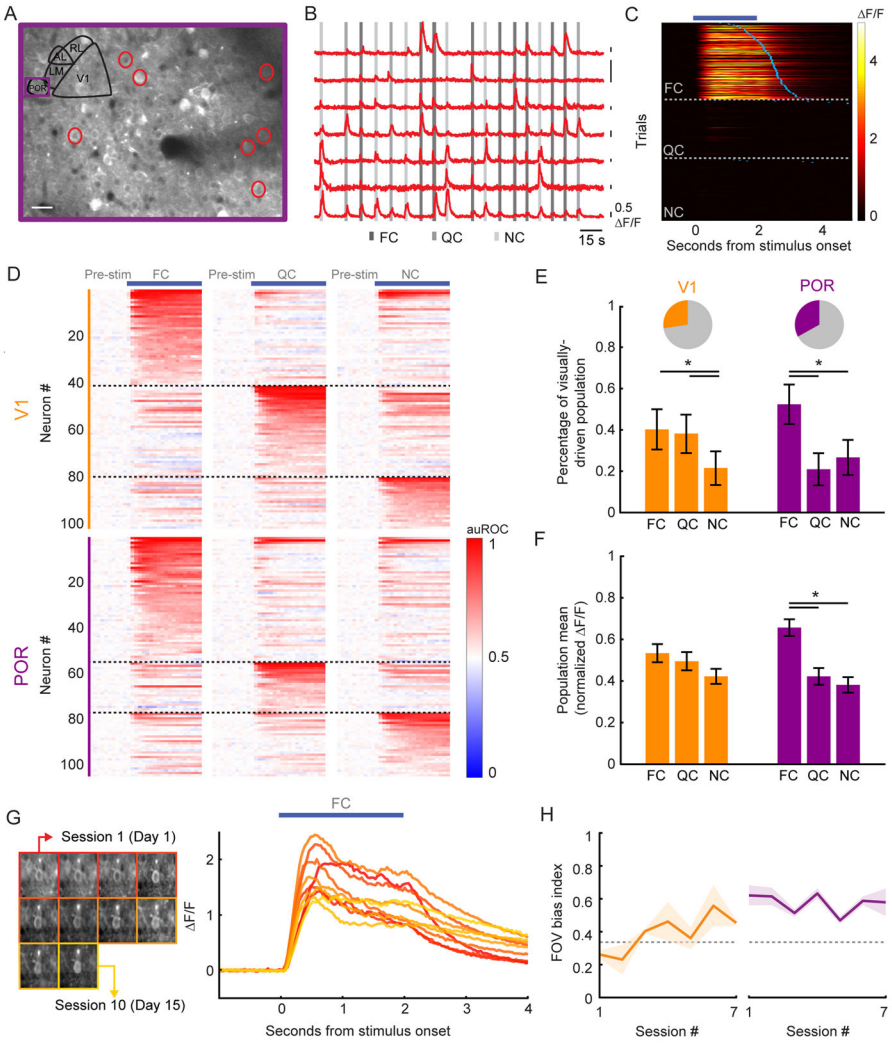

Figure 2. POR, but not V1, demonstrates a response bias to food-associated cues in food-restricted mice

A. Example two-photon image of GCaMP6f expression in POR. Depth: 130 μm.

B. ΔF/F traces from example neurons circled in A. A 50% change in fluorescence (0.5 ΔF/F) is denoted via each black vertical line. Many neurons were responsive to specific visual cues (shaded gray vertical lines).

C. Heatmap of single trial cue-evoked response timecourses (ΔF/F) from an example POR neuron, sorted by visual cue and by latency to first lick (blue ticks). Dark blue bar denotes duration of cue presentation.

D. Normalized auROC timecourses (auROC: area under the receiver operating characteristic) for all significantly driven neurons recorded in V1 and POR. Neurons were sorted according to their preferred cue.

E. Of all recorded cells, 27% in V1 and 33% in POR had a significant cue-evoked response (pie charts). Of these responsive neurons, a significant proportion preferred the FC *vs.* the QC in POR, but not in V1. Errorbars: 95% confidence intervals.

F. By normalizing cellular tuning curves to the largest response and averaging across all responsive neurons, we observed a bias in the mean population response to the FC in POR, but not in V1. Errorbars: SEM across cells.

G. Stable mean food cue-evoked timecourses (*right*) for one example neuron that was recorded in 10 imaging sessions over 15 days (*left*).

H. During each imaging session for each well-trained mouse, we calculated a FC bias index (dashed line at 0.33: no bias towards the food cue) across the field-of-view (FOV). We observed a strong bias towards the FC that was stable across daily sessions in populations of neurons recorded in POR (*right*) but not in V1 (*left*). Errorbars: SEM across animals. *p<0.001, 2-way ANOVA; FC: food cue; QC: quinine cue; NC: neutral cue. Tests on proportions: Tukey's HSD. See also Figures S2–S4.

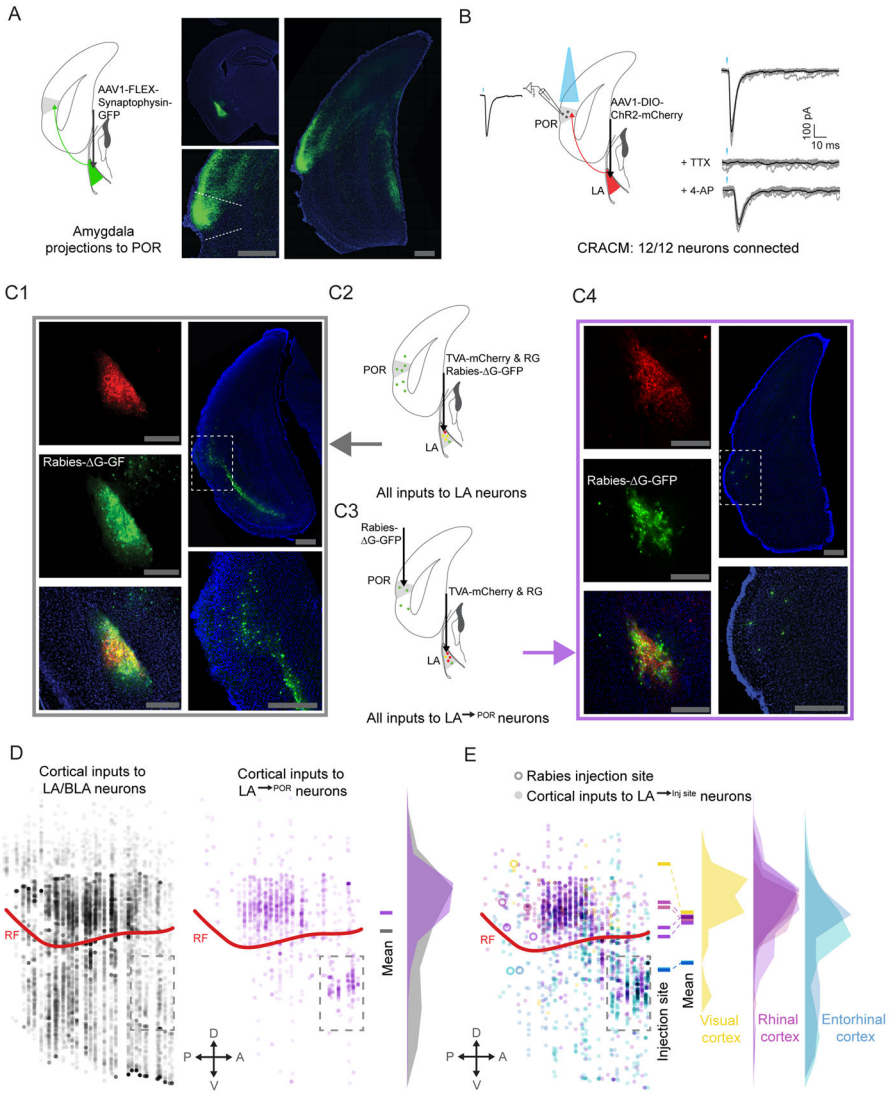

Figure 3. Reciprocal excitatory connectivity between POR and LA

A. Anterograde viral tracing, using cre-dependent AAV-synaptophysin-GFP, demonstrated dense input from LA to POR.

B. *In vitro* ChR2-assisted circuit mapping (CRACM) demonstrated a strong, functional excitatory connection from LA to L2/3 pyramidal neurons in POR (n=12/12). TTX (1 μM) and 4-AP (100 μM) were added to the bath solution in order to confirm monosynaptic connectivity.

C. Rabies-based retrograde tracing was used to characterize inputs to glutamatergic LA neurons, and specifically to $LA^{\rightarrow POR}$ neurons. TVA and rabies glycoprotein were selectively expressed in glutamatergic cells in LA (C1, *top left*) and G-deleted rabies virus was then injected into either LA (C1, *middle and bottom left*) or POR, causing $LA^{\rightarrow POR}$ neurons to selectively be infected (C3 and C4, *middle left and bottom left*). Rabies-tracing (C2) of inputs to all glutamatergic LA neurons showed strong input from many areas in lateral cortex (C1, *right*). Projection-specific rabies tracing (C3–C4) of inputs specific to $LA^{\rightarrow POR}$ neurons also revealed inputs from lateral cortex neurons. Many of these inputs appeared to

be from rhinal cortices (C4, *right*), suggesting a disynaptic, reciprocal excitatory loop from POR to LA and back to POR.

D. Using multi-synapse rabies tracing and whole-brain reconstruction and alignment methods, we confirmed that LA neurons that project to POR received input from a narrower band of neurons in cortex (purple discs), with the greatest density just above the rhinal fissure, in rhinal cortex. Rabies tracing of inputs to all glutamatergic LA neurons (C1–2) demonstrated a larger number and broader distribution of cortical input neurons (gray discs), although the greatest density was still in rhinal cortex.

E. LA projections to different targets in lateral cortex received greater input from cortical regions near the target, suggesting the presence of local, disynaptic reciprocal loops in cortex. Neurons in the immediate vicinity of the LA (dashed rectangle below rhinal fissure) were excluded from analyses in D and E. POR: postrhinal cortex; LA: lateral amygdala; BLA: basolateral amygdala; V1: primary visual cortex; LEnt: lateral entorhinal cortex; rf: rhinal fissure; scale bar: 500 μm. See also Figure S5.

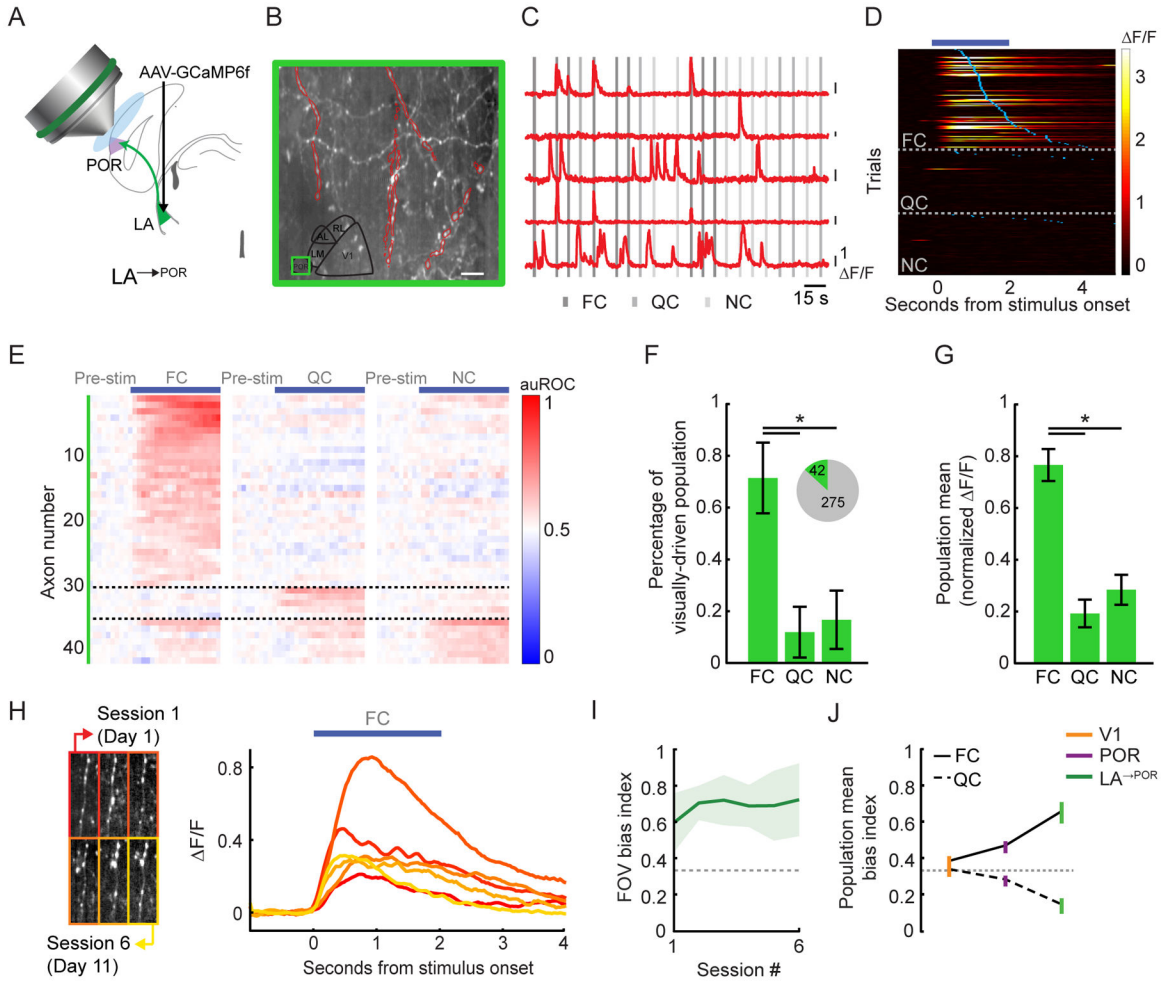

Figure 4. LA feedback axons in POR demonstrate a strong response bias to food-associated cues in food-restricted mice

A. Schematic demonstrating *in vivo* two-photon calcium imaging of LA axons in POR ($LA^{\rightarrow POR}$).

B. Example two-photon image in POR, with a subset of $LA^{\rightarrow POR}$ axons outlined in red.

C. ΔF/F traces from those $LA^{\rightarrow POR}$ axons outlined in B. A 100% change in fluorescence (ΔF/F) is denoted via each black vertical line.

D. Heatmap of single trial cue-evoked response timecourses (ΔF/F) from an example FC-responsive $LA^{\rightarrow POR}$ axon, sorted by visual cue and by latency to first lick (blue ticks). Dark blue bar denotes duration of cue presentation.

E. Normalized auROC timecourses for all significantly driven $LA^{\rightarrow POR}$ axons. Each neuron's responses to all three cues are shown. Neurons are sorted by their preferred cue. Note the high proportion of FC-preferring neurons.

F. We observed a significant visual cue-evoked response in 13% of all recorded $LA^{\rightarrow POR}$ axons (pie charts). Most axons preferred the FC *vs.* the NC or QC. Errorbars: 95% confidence intervals.

G. By normalizing cellular tuning curves to the largest response and averaging across all responsive $LA^{\rightarrow POR}$ axons, we observed a strong bias towards the food cue. Errorbars: SEM across cells.

H. Stable mean FC-evoked timecourses (*right*) for one example axon, recorded across 6 imaging sessions (*left*).

I. During each imaging session for each well-trained mouse, we calculated a FC bias index (dashed line at 0.33: no bias towards the food cue) across the field-of-view (FOV). We observed a reliable population bias towards the FC in $LA^{\rightarrow POR}$ axons across sessions. Errorbars: SEM across animals.

J. Emergence of FC bias from V1 to POR to $LA^{\rightarrow POR}$. Errorbars: SEM across cells. * $p<0.001$, Kruskal-Wallis; FC: food cue; QC: quinine cue; NC: neutral cue. Tests on proportions: Tukey's HSD. See also Figure S6.

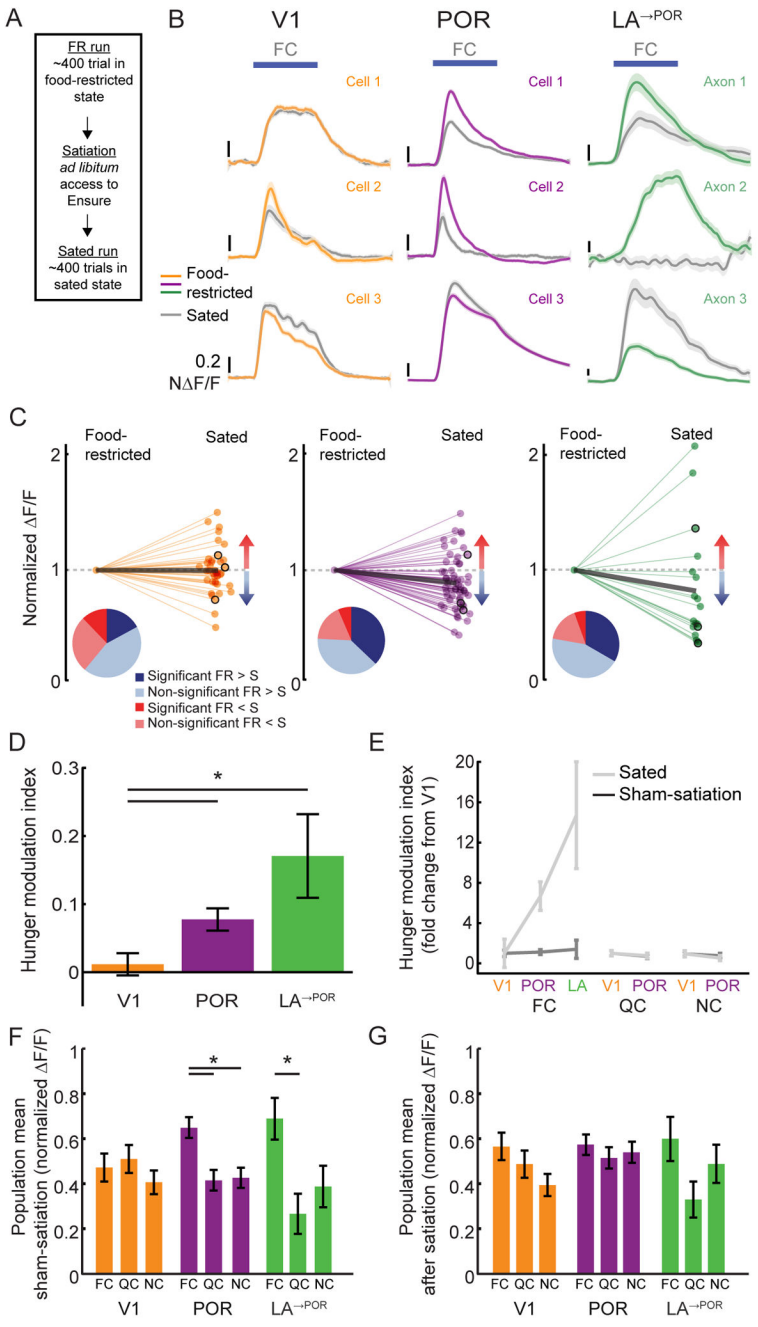

Figure 5. Food cue responses in POR and LA are modulated by hunger state

A. After food-restricted (FR) mice performed ~400 trials of the Go/NoGo visual discrimination task, they were given free access to Ensure (while still head-fixed). Once mice were sated, they received ~400 additional trials (sated hit rate <25%; Figure S1B). In "sham-satiation" sessions, a similar ~45 minute period of time elapsed between early and late sets of trials, during which no Ensure was delivered (Figure S1A).

B. Example traces from V1, POR, and LA$^{\rightarrow POR}$ neuron responses in FR (colored lines) and sated (gray lines) mice.

C. Normalized FC response magnitudes for those neurons that had a significant response to the FC and that were recorded in both FR and sated states. Values less than 1 indicate decreased responses when the mouse was sated. Pie charts illustrate proportions of neurons with responses that were increased (red), decreased (blue), significantly increased (dark red), or significantly decreased (dark blue) by satiation. Data from example neurons from (B) are outlined in black. Thick gray lines: population averages.

D. The average hunger modulation index of FC responses was significantly greater in POR and $LA^{\rightarrow POR}$ neurons than in V1 neurons.

E. The increase in hunger-modulation index values in POR and $LA^{\rightarrow POR}$ neurons (relative to the index value in V1 neurons) observed for the FC was not observed for the QC or NC, or for any cue in sham-satiation sessions.

F. The FC bias in the population mean response in POR and LA (Figures 2F, 4G) persists following the sham-satiation condition.

G. The FC bias was absent following satiation. Errorbars: SEM across cells. * $p<0.05$ 2-way ANOVA; FC: food cue; QC: quinine cue; NC: neutral cue.

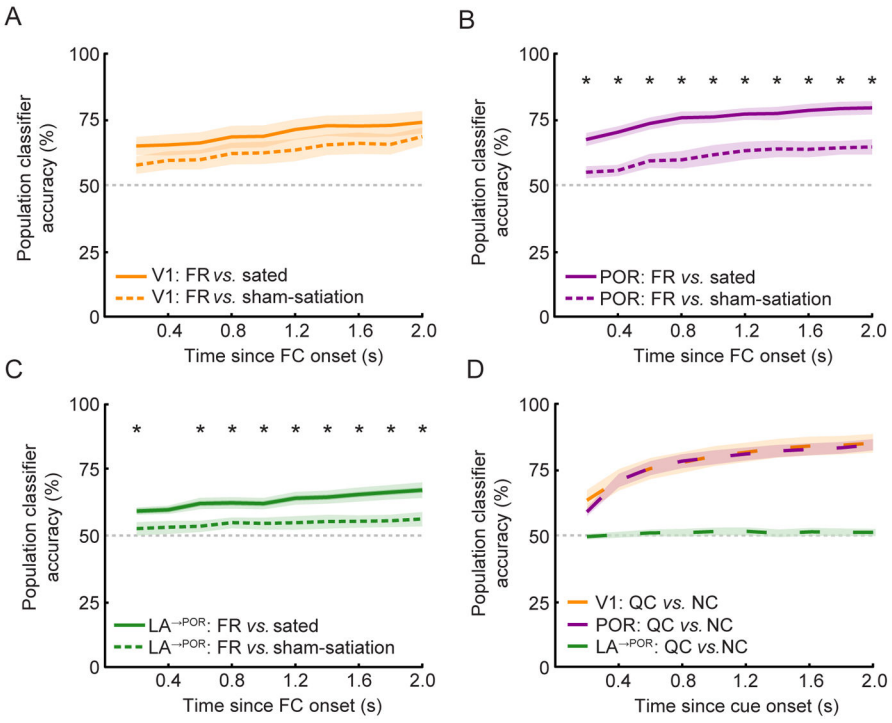

Figure 6. Differential decoding of hunger state *vs.* cue identity from single-trial ensemble activity across areas

A–C. Using single-trial FC responses in simultaneously-recorded populations of neurons, we could correctly predict hunger state with greater than chance (50%) accuracy using a simple linear classifier. In $LA^{\rightarrow POR}$ (C) and POR (B) populations, the classifier performed significantly better in differentiating trials between food-restricted *vs.* sated conditions than between food-restricted *vs.* sham-satiation conditions, while this was not the case in V1 (A), suggesting that hunger state is more strongly represented in POR and $LA^{\rightarrow POR}$ than in V1 populations.

D. By contrast, when discriminating between the identity of two non-rewarded visual cues (QC *vs.* NC), the same classifier performed equally well using population responses of V1 or POR neurons, but at chance levels using population responses of $LA^{\rightarrow POR}$ neurons (due to the low number of QC/NC responsive cells in LA). * $p<0.005$, Wilcoxon Rank-Sum, Bonferroni corrected; Errorbars: SEM. FC: food cue; QC: quinine cue; NC: neutral cue.

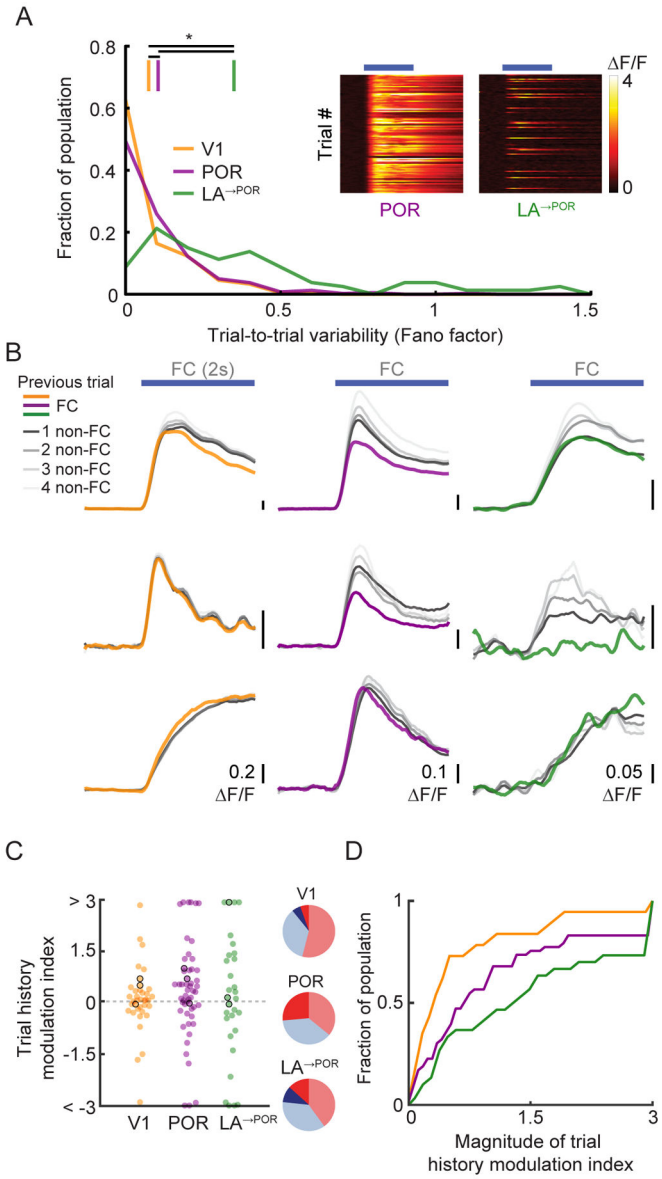

Figure 7. Trial history strongly modulates food cue responses in POR and LA

A. Fano factor, a measure of trial-to-trial variability, increased from V1 to POR to LA$^{\rightarrow POR}$. Insets show single-trial food cue response timecourses from an example POR neuron (*left*) and LA$^{\rightarrow POR}$ axon (*right*) in individual sessions.

B. Single-trial FC responses of V1, POR, and LA$^{\rightarrow POR}$ neurons often depended on trial history. Colored lines represent responses to a FC when preceded by another FC, grayscale lines represent responses to the FC when preceded by one (dark) or many (lighter) non-FCs (QC or NC).

C. Neurons in all three areas showed modulation of FC responses based on trial history, with greater proportions exhibiting large trial history effects in POR and LA$^{\rightarrow POR}$ *vs.* V1. A positive trial history modulation index value indicates greater FC response when preceded by a non-FC. Pie charts show fraction of neurons with positive (red), negative (blue),

significantly positive (dark red) or significantly negative (dark blue) index values. Neurons outlined in black are example neurons from (B). For display purposes, all values >3 or <-3 were set to 3 and −3, respectively.

D. Cumulative distributions of the magnitude of index values, confirming that, as with hunger modulation, V1 neurons showed far less modulation by trial history than POR and $LA^{\rightarrow POR}$ neurons ($p=0.03$, V1 *vs.* POR; $p<0.001$ V1 *vs.* $LA^{\rightarrow POR}$; Kruskal-Wallis).

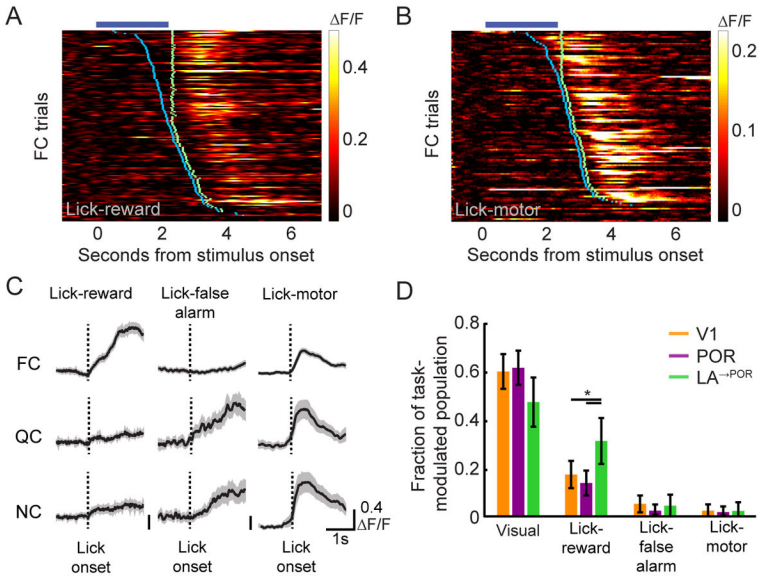

Figure 8. LA$^{\rightarrow POR}$ axons respond to reward in addition to visual cues

A–B. An example LA$^{\rightarrow POR}$ axon that responds post-Ensure delivery, but not to presentation of the FC (A), and an example POR neuron that responds post-licking, but not to presentation of the FC (B). Blue tick marks denote the onset of licking on each trial, while green ticks denote Ensure delivery.

C. Using a general linear model (GLM), we classified subsets of non-cue-responsive yet task-modulated cells, as illustrated by three example neurons from POR (*left column*), LA (*middle column*), and V1 (*right column*). 'Lick-reward' cells selectively increased their activity at lick onset on those trials where the animal correctly licked to presentation of a FC (but not following licking to the QC or NC). 'Lick-false alarm' cells only increased their activity at onset of licking in trials where the animal incorrectly licked to presentation of a QC or NC. 'Lick-motor' cells increased their activity to licking, irrespective of trial type. Errorbars: SEM.

D. While some neurons in V1 and in POR demonstrated non-cue-responsive, task-related responses, a greater proportion of LA$^{\rightarrow POR}$ axons were classified as 'lick-reward.' Errorbars: 95% confidence intervals. We also observed a small incidence of 'multiplexed' cells responsive to both visual and licking events (Figure S6D). * $p<0.05$, Tukey's HSD. FC: food cue; QC: quinine cue; NC: neutral cue. See also Figures S7–8.